Experimental and Theoretical Study of a Direct-Current Arc in an Orifice Nozzle Flow

H. C. Whang* and H. T. Nagamatsu†
Rensselaer Polytechnic Institute, Troy, New York

To increase the basic knowledge about the interaction between an arc near zero current and flows affected by strong shock waves, an investigation was conducted to determine the d.c. arc characteristics at a current of approximately 100 A in an orifice nozzle. Various nozzle pressure ratios were used to produce subsonic and supersonic flows. Cold-flow measurements were used to calculate the arc electrical parameters based on the arc energy integral theory. The calculated results agreed reasonably well with the experimental measurements. It can be concluded that the convection cooling of the arc is the dominant arc cooling process for most currents.

Nomenclature

A = nozzle area
a,b = constants in mass flux equation
C = sonic velocity
C_p = specific heat at constant pressure
E = electric field strength
e = thermal, kinetic, and potential energy per unit mass
h = enthalpy
I = current
j = current density
K = $\sigma[2(h_a-h_c)+(V_a^2-V_c^2)]$
M = Mach number
P = pressure
R = total arc resistance or gas constant
r = radial coordinate
r_0 = arc radius
$R(z)$ = resistance per unit length at z
T = temperature
T_0 = total temperature
U = radiative power
V_a, V_c = velocity of arc and cold-gas flow, respectively
V = arc voltage
w = total arc power
$W(z)$ = power per unit length at z
z = axial coordinate
φ = integration constant
ρ = density
σ = electrical conductivity
γ = specific heat ratio

Subscripts

a = arc plasma flow
c = cold-gas flow

Introduction

THE development of improved high-power gas blast circuit breakers requires basic gasdynamic information on the arc extinction process near zero current. However, many nozzles used in practical circuit breakers do not have shock-free flowfields. The shock waves have strong effects on both average and fluctuating flow velocity.

To investigate the effects of supersonic flows with shock waves on low-current d.c. arcs, a Lexan orifice nozzle with a copper cap was used to produce strong shock waves in supersonic flows. The theoretical background associated with the analysis in this report is based on the method developed by Nagamatsu.[1] Some extrapolations were made on the axial distribution of the flow Mach number and pressure ratio P_s/P_0 for several nozzle pressure ratios. By using the arc equation and Ohm's law, it was possible to obtain the arc radius, electric field strength, voltage, resistance, and power. These calculated results are compared with the experimental measurements with good agreement.

Experimental Apparatus

Orifice Nozzle and Electrodes

An orifice nozzle with a throat diameter of 0.5 in. was constructed out of Lexan polycarbonate resin for electrical insulation as well as for visual observation of the arc at the upstream electrode, as shown in Fig. 1. The upstream 0.5 in. diam electrode, which has a hemispherical nose shape, is made of a copper-tungsten alloy. The downstream electrode is a hollow cylindrical section with a copper-tungsten nosepiece. This electrode is mounted on a movable probe. Both electrodes are adjustable relative to the orifice throat. For the investigations in this paper, the upstream electrode was located 0.05 in. in front of the nozzle entrance and the arc gap distance between the electrodes[2] was 2.17 in.

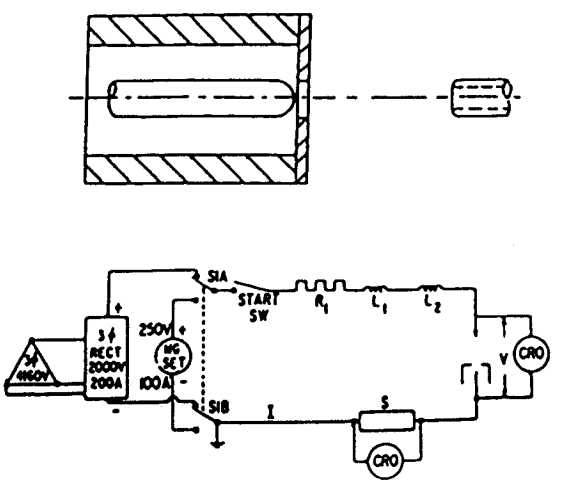

Fig. 1 Schematic of orifice nozzle and electric circuit.

Presented as Paper 83-0399 at the AIAA 21st Aerospace Sciences Meeting, Reno, Nev., Jan. 10-13, 1983; received April 22, 1983; revision received Aug. 15, 1984.

*Graduate Student.
†Professor of Aeronautical Engineering. Fellow AIAA.

Flow System

High-pressure air is supplied either by a 200 hp compressor at 7.8 bar or by an 800 hp compressor at 35 bar. Both of these compressors are connected in parallel with valves through a 2.0 in. diam, 500 psi piping system. A large storage tank is connected to the discharge from these compressors. A Fisher control valve, located upstream of the 6.0 in. diam reservoir section, is used to regulate the supply pressure. The temperature of the air supply is near room temperature. The gas discharges downstream from the nozzle into a duct exhausting to the outside.[1,2]

Power Supply

A schematic diagram of the power supply circuit is shown in Fig. 1. A 250 V motor generator set or a 2000 V rectified system[2] supplies d.c. current to the arc through the network represented in Fig. 1. One side of the generator is grounded and an external resistance of 1.4 Ω is connected in series to limit the current to 150 A. The current for the 2000 V rectified power supply is varied by adjusting the resistance in the electrical circuit as shown in Fig. 1. After the flow is established in the nozzle, the switch is closed for approximately 500 ms and the steady d.c. arc is established in approximately 40 ms.

Arc Energy Integral Theory

Assumptions

A theoretical analysis has been developed by Nagamatsu[1] to examine the behavior of arcs under quasistationary, convection-dominated conditions. To simplify the analysis of the arc, the following assumptions were made: 1) steady and axial symmetrical uniform flow, $\partial/\partial t=0$ and $\partial/\partial r=0$; 2) radial pressure variation is neglected, $\partial p/\partial r=0$; 3) arc temperature is constant and independent of radius and axial distance; 4) axial and radial heat conduction is negligible compared with convection, $\partial T/\partial r=0$ and $\partial T/\partial z=0$; and 5) local thermodynamic equilibrium is maintained.

The arc and the cold flow are represented by the two-zone model shown in Fig. 2, with the constant arc temperature and cold flow determined by the nozzle geometry, adiabatic flow, and nozzle pressure ratio.

The Arc Equation

Applying conservation of mass and energy to the control volume of a differential element of the arc (Fig. 2), the steady-state energy balance yields

$$(\sigma E^2-U)r_0^2\mathrm{d}z=\rho_c V_c[2(h_a-h_c)+(V_a^2-V_c^2)]r_0\mathrm{d}r_0 \quad (1)$$

The right-hand side represents the energy associated to heat the cold-gas flow to the arc temperature and the kinetic energy required to accelerate the cold-gas flow to the arc velocity. The experimental data of Hermann et al.[3] stated that, near zero current, the radiation term U can be neglected compared to the ohmic heating term σE^2.

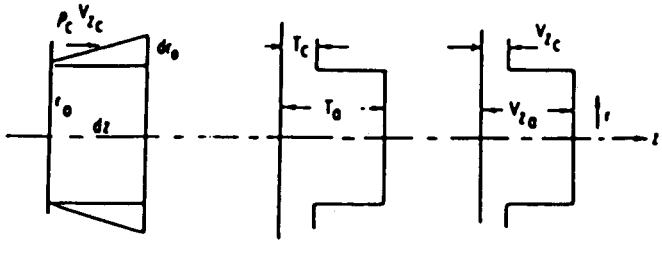

Fig. 2 Two-zone channel flow model and coordinate system.

Therefore, Eq. (1) can be written as

$$\sigma E^2 r_0^2\mathrm{d}z=\rho_c V_c[2(h_a-h_c)+(V_a^2-V_c^2)]r_0\mathrm{d}r_0 \quad (2)$$

Ohm's law relates the current to the electric field strength by

$$j=\sigma E \quad (3)$$

The current is given as

$$I=\int_A j\mathrm{d}A=\pi r_0^2\sigma E \quad (4)$$

The electric field strength can be written as

$$E=I/\pi r_0^2\sigma \quad (5)$$

Substituting Eq. (5) into Eq. (2) yields

$$(I^2/\sigma\pi^2)\mathrm{d}z=\rho_c V_c[2(h_a-h_c)+(V_a^2-V_c^2)]r_0\mathrm{d}r_0 \quad (6)$$

A factor K is introduced and is determined by

$$K=\sigma[2(h_a-h_c)+(V_a^2-V_c^2)] \quad (7)$$

The differential equation for the arc can be rewritten as

$$\frac{\mathrm{d}z}{\rho_c V_c}=\frac{\pi^2}{I^2}Kr_0^3\mathrm{d}r_0 \quad (8)$$

It is shown in the calculations that the factor K is approximately constant because the arc enthalpy h_a is very large and is approximately constant.

Solution of the Arc Equation

To integrate Eq. (8), it is necessary to know the variation of the cold-flow mass flux $\rho_c V_c$ as a function of the axial distance z. This function can be found from the cold-flow mass flux distribution plot by a piecewise linear approximation.

From the experimental pressure measurements[1,4] of the 0 and 4 deg convergent-divergent nozzle and the orifice nozzle, it is reasonable to assume that the downstream of the nozzle has constant mass flux. The linear equation of mass flux is given by

$$\rho_c V_c=a_1 z+b_1, \qquad z_0\le z\le z_1 \quad (9a)$$

$$\rho_c V_c=a_2 z+b_2, \qquad z_1\le z\le z_2 \quad (9b)$$

$$\rho_c V_c=b_3, \qquad z_2\le z\le z_e \quad (9c)$$

where z_0 is the upstream electrode location, z_1 the maximum mass flux location, z_2 the location of the constant mass flux, and z_e the downstream electrode location.

The a and b in Eqs. (9) are constants and need to be determined from the axial mass flux distribution.

By substituting the linear variation of the cold-flow mass flux [Eqs. (9)] into Eq. (8), the arc radius for each region can be found,

$$r_{0_1}=\left\{\frac{4}{K_1}\left[\frac{I^2}{\pi^2}\frac{1}{a_1}\ln(a_1 z+b_1)+\varphi_1\right]\right\}^{1/4}, \qquad z_0\le z\le z_1 \quad (10a)$$

$$r_{0_2}=\left\{\frac{4}{K_2}\left[\frac{I^2}{\pi^2}\frac{1}{a_2}\ln(a_2 z+b_2)+\varphi_2\right]\right\}^{1/4}, \qquad z_1\le z\le z_2 \quad (10b)$$

$$r_{0_3}=\left\{\frac{4}{K_3}\left[\frac{I^2}{\pi^2}\frac{1}{b_3}\cdot z+\varphi_3\right]\right\}^{1/4}, \qquad z_2\le z\le z_e \quad (10c)$$

where the subscript on K indicates the average value over each region, and the φ are the integration constants. In region 1, the value of φ_1 is assumed to be zero, which has been proved to have a very satisfactory result compared with the experimental data in 0, 4, and 15 deg convergent-divergent nozzles.[1,4,5] The values of φ for the other two regions can be found by requiring that the arc radius be continuous along the nozzle axis. That is,

$$\varphi_2 = \frac{K_2}{K_1}\left[\frac{I^2}{\pi^2}\frac{1}{a_1}\ln(a_1 z_1 + b_1) + \varphi_1\right] - \frac{I^2}{\pi^2}\frac{1}{a_1}\ln(a_2 z + b_2) \tag{11a}$$

$$\varphi_3 = \frac{K_3}{K_2}\left[\frac{I^2}{\pi^2}\frac{1}{a_2}\ln(a_2 z_2 + b_2) + \varphi_2\right] - \frac{I^2}{\pi^2}\frac{z_2}{b_3} \tag{11b}$$

The electric field strength E as a function of z for each region of the arc can be found by using Eq. (5) and Eqs. (10) for the arc radius. The relation is given by

$$E_1 = \left\{\frac{K_1 a_1}{4\sigma^2[\ln(a_1 z + b_1) + \varphi_1(\pi^2 a_1/I^2)]}\right\}^{1/2}, \quad z_0 \le z \le z_1 \tag{12a}$$

$$E_2 = \left\{\frac{K_2 a_2}{4\sigma^2[\ln(a_2 z + b_2) + \varphi_2(\pi^2 a_2/I^2)]}\right\}^{1/2}, \quad z_1 \le z \le z_2 \tag{12b}$$

$$E_3 = \left\{\frac{K_3}{4\sigma^2[(z/b_3) + \varphi_3(\pi^2/I^2)]}\right\}^{1/2}, \quad z_2 \le z \le z_e \tag{12c}$$

where the value of electrical conductivity σ, which is taken from Ref. 7, varies with the axial distance. It is interesting to note that the electric field strength E is independent of current for the assumed two-channel flow model. Because σ is proportional to I^2, current can be cancelled out of the equation.

The arc voltage at any axial position z can be found by integrating the electric field strength from Eq. (12) with respect to the axial distance and is given by

$$_1V_2 = \int_{z_1}^{z_2} E(z)\,dz \tag{13}$$

The total arc voltage is found by integrating the electric field strength from the upstream electrode location to the downstream electrode location. The arc resistance per unit length is given by

$$R(z) = E(z)/I \tag{14}$$

and the arc power per unit length by

$$W(z) = E(z)I \tag{15}$$

Cold-Gas Flow

The continuous flow through the orifice nozzle is assumed to be inviscid with uniform flow across the nozzle cross section. It is also assumed that the gas is calorically perfect so that the specific heats are constant and there is no heat conduction at the nozzle walls. The total temperature T_0 of the cold flow is assumed to remain constant at room temperature. The static temperature T along the nozzle axis can be calculated[6] and the cold-flow enthalpy is given by

$$h_c = C_p T \tag{16}$$

Based on the calculated flow velocity and density, the cold-flow mass flux $\rho_c V_c$ as a function of the axial distance can be found.

Arc Plasma Flow and Properties

By the assumption of inviscid and isothermal processes, the equation of motion for the plasma is given by

$$V_a \cdot \frac{\partial V_a}{\partial z} = -\frac{1}{\rho_a}\frac{\partial p_a}{\partial z} \tag{17}$$

The plasma static pressure is assumed to be equal to the cold-flow static pressure. The plasma temperature approximately equals a constant, which is around 20,000 K. The plasma density can be expressed as

$$\rho_a = p_a/RT_a \tag{18}$$

By substituting this equation into Eq. (17) and integrating, the plasma velocity is given by

$$V_a = \left[\frac{2}{RT_a}\ln\left(\frac{p_u}{P}\right) + V_{au}^2\right]^{1/2} \tag{19}$$

where the subscript u indicates the conditions at the upstream electrode. The upstream arc velocity is assumed to be equal to the local cold-flow velocity.

Under the assumption of local thermodynamic equilibrium, the air and nitrogen plasma enthalpy and electrical conductivity as a function of static pressure at temperature of 20,000 K were calculated by Yos.[7]

Experimental and Extrapolated Cold-Flow Data

The ratio of static pressure to reservoir pressure of cold-gas flow along the axial distance is measured for a nozzle pressure ratio of 2.36. From this, the flow Mach number and the mass flux along the axial distance can be calculated. For all other nozzle pressure ratios, the flow Mach numbers along the axial distance were found by extrapolating the measured data from the schlieren photographs and laser velocimeter measurements.[2] These will be discussed in more detail in the following subsections.

Experimental Data of a 2.36 Nozzle Pressure Ratio

For a nozzle pressure ratio of 2.36, the ratio of static pressure to reservoir pressure of cold-gas flow P_s/P_0 as a function of axial distance is obtained from the experimental data of Ref. 2. The pressure ratio P_s/P_0 increased at the beginning to a peak value near the nozzle throat and then decreased monotonically to the downstream before the shock bottle occurred. From the static and impact pressure data taken along the nozzle axis, the local flow Mach number distribution can be determined by the Rayleigh-Pitot formula. The result is presented in Fig. 3.

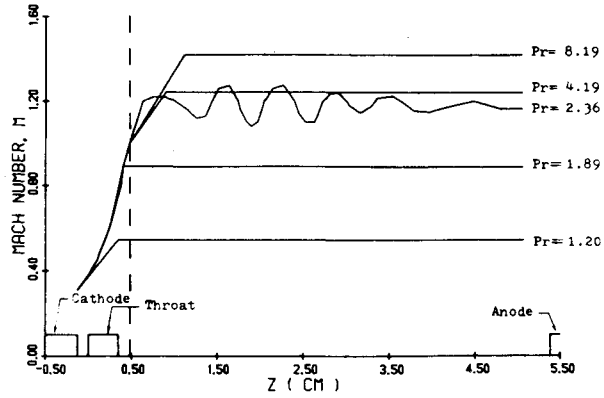

Fig. 3 Flow Mach number for orifice nozzle as a function of axial distance and pressure ratio.

Extrapolated Flow Mach Number and Static Pressure Distribution for all Other Nozzle Pressure Ratios

For all other nozzle pressure ratios, the approximated location of the maximum Mach number can be found from the schlieren photographs.[2] These pictures show that the shock bottle location moves downstream as the nozzle pressure ratio increases. The approximated maximum flow velocity can be found from Fig. 4 where the mean flow velocity is measured by the laser velocimeter on the axis 1 in. from the orifice exit.[2] By assuming that the total flow temperature is equal to room temperature, the local flow temperature and local sound speed can be found.[6] Thus, the local flow Mach number can be determined. These extrapolated results of the flow Mach number are shown in Fig. 3. The vertical reference line in this figure shows the location of Mach 1 for nozzle pressure ratios of 2.36, 4.19, and 8.19.

Arc Calculations and Correlation with Experimental Data

Arc and Cold-Flow Velocity

From the flow Mach number and static pressure data, both the arc and cold-flow velocities can be found by using Eq. (19) and the adiabatic equation.[6] The results of these calculations are presented in Fig. 5. At a nozzle pressure ratio of 2.36, the static pressure and flow Mach number distributions are obtained from experimental measurements. The axial flow Mach number fluctuates through each shock bottle. Consequently, the arc and cold-flow velocities also fluctuate. Because of the assumption of the extrapolation that the flow Mach number remains constant after the maximum Mach number location, the arc and cold-flow velocities do not fluctuate at other nozzle pressure ratios.

Mass Flux Linear Approximations

The cold-flow mass flux was calculated and the results are presented in Fig. 6 for various nozzle pressure ratios. The actual mass flux distributions fluctuate because of the shock bottle effect. However, the linear approximations represented by the dashed lines were used in the arc energy integral method.

Arc Radius

Under the assumption of the integration constant $\varphi_1 = 0$, which has been proved to be in good agreement with experimental data for convergent-divergent nozzles,[1,4,5] the arc radius can be calculated as a function of z by using Eq. (10). The results for the various nozzle pressure ratios are presented in Fig. 7. From this figure, it is found that the arc radius varies nearly linearly with axial distance z despite the complicated functional form and decreases with increasing nozzle pressure ratio.

Electric Field Strength

From Eq. (5), the electric field strength was calculated at various axial positions by using the local values of the electrical conductivity and arc radius. The results are presented in Fig. 8. For nozzle pressure ratios greater than 1.89, the electric field strength first decreases and then increases before the location of Mach 1 and it decreases monotonically with the axial distance afterward. This is caused by the rapid changes of the static pressure. Hence, from Eq. (5), the elec-

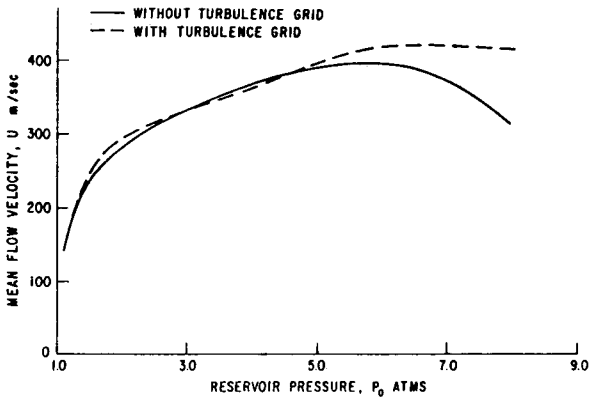

Fig. 4 Mean flow velocity for orifice nozzle as a function of reservoir pressure with and without turbulence grid.

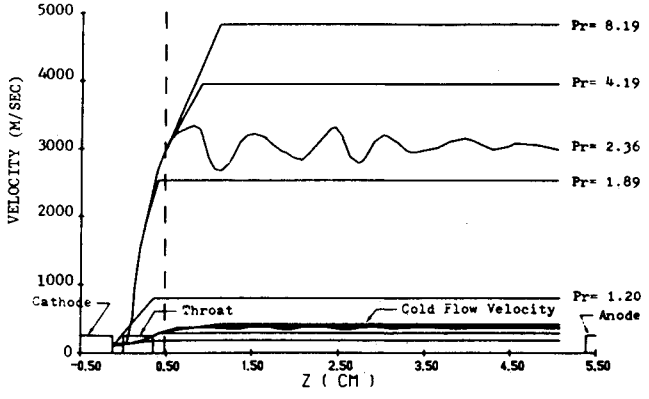

Fig. 5 Arc and cold-flow velocities as functions of axial distance and pressure ratio.

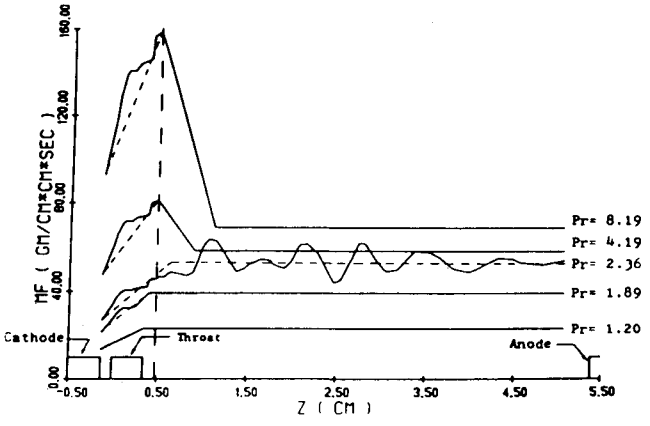

Fig. 6 Flow mass flux for orifice nozzle as a function of axial distance and pressure ratio.

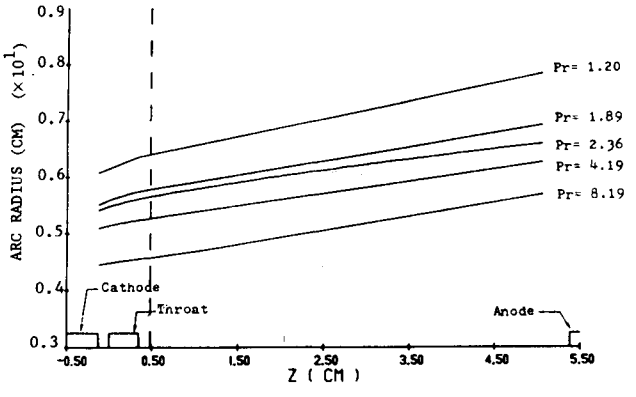

Fig. 7 Arc radius as a function of axial distance and pressure ratio.

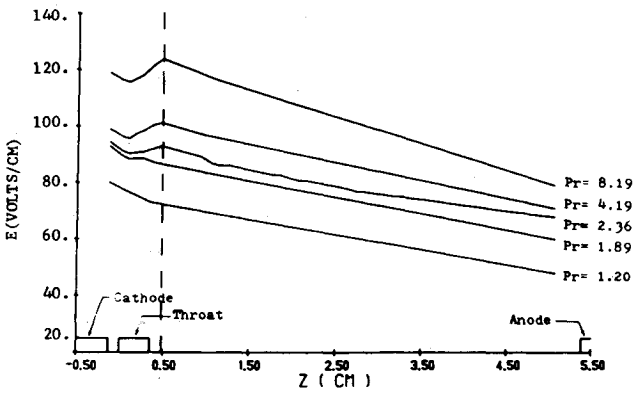

Fig. 8 Electric field strength as a function of axial distance and pressure ratio.

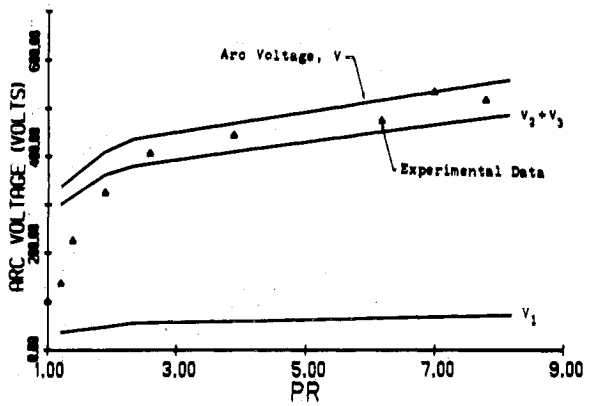

Fig. 9 Arc voltage as a function of pressure ratio.

tric field strength has a local peak value at the location of Mach 1.

Arc Voltage

The arc voltage can be found by integrating the electric field strength found previously. The total arc voltage as a function of nozzle pressure ratio is shown in Fig. 9, as are the arc voltages V_1, V_2, and V_3 of regions I, II, and III. The calculated arc voltages have satisfactory results compared with the experimental data[2] represented by the triangle symbols.

Arc Power and Resistance

The arc power is found by multiplying the arc voltage by the current. The resistance is found by dividing the arc voltage by the current. Since the current was nearly constant throughout the experiment, the curves for arc power and arc resistance will show the same trends as exhibited in Fig. 9.

Shock Wave Effects

The orifice nozzle has a characteristic, well-known structure of flowfield, as seen in the schlieren photographs.[2] The shock bottles, with the associated strong changes in density and velocity caused by the inertia of the gas expanding from the orifice to the ambient pressure, are visible in the supersonic flow region.

The flow Mach number decreases and the static pressure increases after the shock wave. Increased pressure reaccelerates the flow in the shock bottle. Therefore, the axial Mach number fluctuates through these shock bottles at supersonic velocities.[8] As a result, the static pressure also fluctuates. Consequently, this leads to a fluctuating mass flux along the axis. The comparison of the experimental arc voltage data[1,4] of the orifice nozzle with the 0 and 4 deg convergent-divergent nozzles has shown that, for higher pressure ratios, the orifice nozzle has lower voltage values than the others. This is primarily due to the influence of strong shock bottle that occurs for the orifice nozzle at the higher pressure ratios. These strong shock waves rapidly decrease the cold flow and the plasma velocity and increase the static pressure and the electrical conductivity.[9] These phenomena cause a decrease in the arc voltage.

Discussion and Conclusions

Because of the choked flow condition, the Mach number and the static pressure ratio P_s/P_0 distribution along the axis from the upstream electrode to the throat remained nearly the same for nozzle pressure ratios greater than 1.89. In this region, only the cold-flow density is increased with the reservoir pressure in the nozzle. In this study, the flow Mach number and pressure ratio distributions before Mach 1 location for the nozzle pressure ratios of 1.89, 4.19, and 8.19 are taken to be the same as for the nozzle pressure ratio of 2.36.

For the nozzle pressure ratios of 4.19 and 8.19, the flow Mach number should fluctuate because of the presence of the shock bottles as shown in the schlieren photographs. The variation in the Mach number increases as the nozzle pressure ratio increases.[10] In this study, it is assumed that the fluctuating Mach number portion is equal to a constant, an assumption based on laser velocimeter measurements due to the lack of experimental data. This assumption introduces some error in the calculated arc properties.

The maximum values of mass flux for nozzle pressure ratios of 4.19 and 8.19 occur at the Mach 1 location. Downstream from the Mach 1 location, the mass flux decreases as the flow accelerates to supersonic velocities. This is due to the fact that the static pressure and density continuously decrease in the supersonic region.

In Eq. (10), if a positive value is chosen for the constant of integration φ_1, the arc radius is increased and the electric field strength and arc voltage are decreased. If a negative value is chosen for φ_1, it has the reverse effects.

It is evident from Fig. 7 that the arc diameter decreases drastically as the flow velocity increases (i.e., increasing the nozzle pressure ratio with ambient pressure downstream of the nozzle). This demonstrates that a strong arc constriction exists in the flowfield. Strong arc constriction with increasing flow velocity leads to very high current densities in the gas blast interrupters.

The calculated arc voltages, resistances, and powers for a current of approximately 100 A compare favorably with the measured values. Thus, it can be concluded that the energy balance of the ohmic heating and convective cooling of the arc is the dominant cooling process for most currents.

In the future, a more accurate analysis could be made by taking into account radiation, conduction heat transfer, and variation of the arc temperature with radius and axial distance. Also, the direct measurement of static pressure and flow Mach numbers can result in a more accurate calculation for the arc properties.

Acknowledgments

The authors wish to extend special thanks to R. E. Sheer Jr., J. R. Bowden, G. Frind, R. E. Kinsinger, and F. F. Ling, who helped to make this paper possible. The funding of the experimental work by General Electric Company and Electric Power Research Institute is also gratefully acknowledged.

References

[1]Nagamatsu, H. T., "Experimental and Theoretical Study of a D.C. Arc in a Constant Diameter Nozzle Flow," IEEE Paper 81 SM 468-8, July 1981.

[2]Benenson, D. M., Frind, G., Kinsinger, R. E., Nagamatsu, H. T., Noeske, H. O., and Sheer, R. E. Jr., "Fundamental Investigation of Arc Interruption in Gas Flows," Electric Power Research Institute EL-1455, July 1980.

[3]Hermann, W., Kogelschatz, U., Niemeyer, L., Ragaller, K., and Schade, E., "Experimental and Theoretical Study of a Stationary High-Current Arc in a Supersonic Nozzle Flow," *Journal of Physics D: Applied Physics*, Vol. 7, 1974.

[4]Nagamatsu, H. T. and Symolon, P. D., "An Experimental and Theoretical Study of a D.C. Arc in an Eight Conical Nozzle Flow," AIAA Paper 81-0097, Jan. 1981.

[5]Nagamatsu, H. T. and Scavallo, P. G., "An Experimental and Theoretical Study of a D.C. Arc in a 30 Conical Nozzle Flow," AIAA Paper 80-0092, Jan. 1980.

[6]NASA Ames Research Staff, "Equations, Tables, and Charts for Compressible Flow," NASA TR 1135, 1955.

[7]Yos, J. M., "Transport Properties of Nitrogen, Hydrogen, Oxygen and Air to 30,000 K," Avco, Technical Memo RAD-TM-63-7, 1963.

[8]Liepmann, H. W. and Roshko, A., *Elements of Gasdynamics*, John Wiley & Sons, New York, 1957.

[9]Von Engel, A., *Ionized Gases*, Clarendon Press, Oxford, England, 1955.

[10]Frind, G., Kinsinger, R. E., Miller, R. D., Nagamatsu, H. T., and Noeske, H. O., "Fundamental Investigation of Arc Interruption in Gas Flows," Electric Power Research Institute Rept. EPRI EL-284, Jan. 1977.